Molecular Activation Energies ($\Delta\mu_2^*$) of L-Lysine, L-Tyrosine, L-Proline, DL-Alanine, Glycerol, Orcinol, Iodine, DTAB, and TMSOI for Blending with Melamine-Formaldehyde-Polyvinylpyrrolidone Polymer Resin Illustrated with SEM

Man Singh,[1,2] Vinod Kumar,[1,3] R. K. Kale,[2] C. L. Jain[3]

[1]*Chemistry Research Lab, Deshbandhu College, University of Delhi, New Delhi 110019, India*
[2]*School of Chemical Sciences, Central University of Gujarat, Gandhinagar 382030, Gujarat, India*
[3]*Department of Chemistry, MMH College, CCSU, Meerut, Uttar Pradesh, India*

Received 4 November 2009; accepted 14 March 2010
DOI 10.1002/app.32457
Published online 27 May 2010 in Wiley InterScience (www.interscience.wiley.com).

ABSTRACT: Efficient molecular mixing together is a key precondition for industrial exploitation of individual macromolecules for potential product development and quality assurance with resource saving mechanism. Conceptually, MFP (melamine-formaldehyde-polyvinylpyrrolidone) polymer resin was mixed with amino acids (L-lysine, L-tyrosine, L-proline, DL-alanine), nonionic surfactants (glycerol, orcinol), iodine as metal and cationic surfactants (DTAB, TMSOI) as dispersants, in 4 : 1 ratio, w/w. A mutual molecular dispersion occurs at a cost of molecular activities with utilization of a sufficient amount of activation energies. The activation energies ($\Delta\mu_2^*$, kJ mol^{-1}) were derived from intrinsic viscosities ([η], kg/L) and partial molar volumes ($\overline{V}_2$, 10^{-6} m^3/mol), which were calculated from experimental data of viscosities (η, N s m^{-2}) and apparent molar volumes (V_2, 10^{-6} m^3/mol) of 0.005, 0.007, 0.009, and 0.0011 g/mL aqueous samples of the dispersants at 304.15 K. The limiting data were fitted to standard activation energy equations and were analyzed to assess potential of their micromixing. Densities ($\rho/10^3$ kg m^{-3}) for apparent molar volume ($V_2/10^{-6}$ m^3 mol^{-1}) and viscosity (η, $0.1N$, s m^{-2} = 0.1 kg m^{-1} s^{-1}, = 1 poise, SI unit) were also measured with weight method. The $\Delta\mu_2^* < 0$, in arrange of −48.35 to −118.03 kJ/mol were noted that inferred effective micromixing evidenced with SEM images of the blends. The $\Delta\mu_2^*$, kJ mol^{-1} data are as glycerol (−118.03) > TMSOI (−117.55) > DTAB (−102.93) > orcinol (−101.54) > MFP-R (−93.71) > iodine (−59.32) > L-proline (−59.27) > L-lysine (−55.87) > DL-alanine (−55.04) > L-tyrosine (−53.04) > water (−48.35) orders with maximum utilization of $\Delta\mu_2^*$, glycerol. © 2010 Wiley Periodicals, Inc. J Appl Polym Sci 118: 960–968, 2010

Key words: intermolecular forces; viscosity; partial molar volume; activation energy; micromixing

INTRODUCTION

On blending and mixing, the molecules undergo several critical changes to optimize a bulk structure of resultant products because the blending is obtained by mechanical mixing. The dissolution is another phenomenon where a solute is dissolved in bulk amount of the solvent with structural interactions. In case of the mixing or blending such structural interactions may not occur and only dispersion of molecules mutually takes place.[1,2] In dissolution, the solvent energy is utilized and also an activation of solute contributes to a phenomenon but the blending is done due to activation energy of both the molecules to be mixed mutually.[3] The molecular oscillations in a repetitive vibrational mode about a central point of equilibrium between two or more different states are not very effective for micromixing[4] but with vibration due to mechanical oscillation with vibrational energy $E_v = (v + 1/2)\ h\nu_0$, cause favorable mixing. The $v = 0, 1, 2, n.$ are vibrational quantum numbers and total molecular energy (E_{mol}) is constituted of electronic, vibrational, rotational, nuclear, and translational components with many degree of freedom that lead to micromixing. The E_{mol} is given as later

$$E_{mol} = E_{electronic} + E_{vibrational} + E_{rotational} + E_{nuclear} + E_{translational}$$

The $E_{electronic}$ is electronic or a potential energy surface at equilibrium geometry and energies of these components vary with the oscillations. The atoms and ions, in bound state develop interatomic forces due to consistent vibrations away from equilibrium position.[5] Elastic waves of different lengths,

Correspondence to: M. Singh (mansingh50@hotmail.com).
Contract grant sponsors: University Grants Commission, Government of India.

frequencies and amplitudes run through crystalline solids with atomic vibrations frequencies of 10^{13} Hz and the 10^{-11} m amplitude.[6] Such atomic vibrations are important for metallic, covalent, ionic crystals, semiconductors, intermetallic compounds, and interstitial phases.[7] These theories are applied to our mixing studies because intrinsic energy levels or orbital state energy level of an electron in atomic orbital determines electrostatic interaction with energy levels around a nucleus is as $E_n = -hcRZ^2/n^2$. The R is Rydberg constant, Z is atomic number, n is principal quantum number, h is Planck's constant, and c is a speed of light. A structural splitting arises from spin-orbit coupling and Darwin term interaction of s-shell electrons inside the nucleus.[8] Electron transfer is a biggest link for linkage intermolecular basis that lead to transformations. Johan Dalton's atomic theory for chemical combinations configures interacting molecules, for reorientation is on mass and potential scales.[9] The field of microfluidics research is still relatively relevant and currently going through a period of intense development, especially in the areas of analytical chemistry and diagnostics for which its principle applications were originally intended for physicists.

EXPERIMENTAL

Materials and methods

The melamine-formaldehyde-polyvinylpyrrolidone (MFP) preparation, structural, and physicochemical study are reported in our previous work where pure melamine (E. Merck), formaldehyde 40% (E. Merck), and PVP (E. Merck) were used.[10] The iodine (Merck), DTAB, orcinol (Sigma), TMSOI, DL-alanine, L-proline, L-lysine, L-tyrosine (Spectrochem), glycerol (Qualigens) were used as received. The mixing was made under similar experimental conditions with preweighed amounts of hot melts of MFP with prescribed amounts of the additives in 4 : 1 ratio, w/w, with $\pm 1 \times 10^{-5}$ g accuracy 100 DS Dhona balance, Instruments Pvt, Calcutta India. Each additive was blended separately with the MFP and mixed to a homogenous state with a flat tipped glass stirrer fitted to a wiper motor, ran at a rate of 80 rpm. The blending was mad to introduce degradable properties in resultant products. The resin in a paste state was taken in Borosil glass made boiling tube or cell of 15 cm in length and a 2 cm radius (r) or a 4 cm inner diameter, with $\pi r^2 h$ capacity. The $r = 2$ cm and $h = 15$ cm, with 188 cm^3 cell volume. The contents were shaken for 5 to 8 h at a rate of 80 rpm using wiper motor till it produced a homogenous mixture at NTP. Thermodynamic parameters entropy etc, were varied with no color change except the orcinol and iodine. The blends were stored in P_2O_5 filled desiccator. The orcinol, a phenolic in nature, gave yellowish color with MFP and the iodine detained color. The MFP structures were suited for blends with L-lysine, L-tyrosine, L-proline, DL-alanine, glycerol, orcinol, iodine, DTAB, and TMSOI because of similarity in electronic motions whereby physicochemical bonds were established to form a product to be used in electronic, thermal stability, tensile strength, porosity.

Interesting chemistry of blending

The purpose of this study was to find out an interesting chemistry of useful blends prepared out of the MFP resin and amino acids along few industrial surfactants. The studies were intensified to find out the blending potential in terms of the individual molecular activation energies and their respective SEM micrographs. The choice of blending of zwitterionic structures with MFP must not be misunderstood by surface coating or sputtering coat. The purpose of the study was to find out possibilities of mutual mixing of the amino acid a resin, and hence attention is required on the sole motto of the studies, which was to investigate mixing or blending potential for industrial uses and developing smart composites. Hence the activation energies of individual additive and the SEM of their blends are studied as the SEM authentically reveals internal structural reorientations of amino acids along thermodynamics of their mixing potential with the resin.

MFP resin + additive blends sample preparation

The samples were prepared with hot melt of the freshly prepared resin in 4 : 1 ratios, w/w.[10] The resin sample was transferred into a borosil glass made sample container of 60×20 $(mm)^2$ dimensions of length and width, respectively. The prescribed amounts of the additives was cautiously added with the resin in the container and smoothly mixed together for 10–20 min. The mixing was made with specifically designed glass stirrer fitted with wiper motor to control the rpm. Initially, the 50–100 rpm was maintained for 20 min but latter it was raised to 150–200 rpm for 2–3 h. The rpm was cautiously control not to generate a mechanical heat in the mixture but allow distribution and dispersion of the molecules together. The mixing was continued till Boltzmann energy distribution factor $e^{-E/KT}$, developed an energetic equilibrium in the mixture and hence a novel combination of molecular activation energy and SEM microstructure was proposed. The mixing and mixing operation was worked out in a close environment of Perspex sheet made box of 80×70 cm^2 dimensions of length and width, respectively. The SEM of sample was recorded after each 20 min,

when mixing was made. When a homogenous microstructure was noticed in SEM then the mixing was stopped and the samples were stored in P_2O_5 filled vacuum dessicator.

Scanning electron microscope

The SEM images were recorded with ZEISS EVO Series Scanning Electron Microscope (SEM) EVO 50, for topographic and microstructural analysis. The details of SEM characterization are noted for finding structural signatures of the blends with molecular activation energies ($\Delta\mu_2^*$) of the additives. The purpose was not to focus SEM instrumentation but to apply the technique illustrat the thermodynamics of blending, explained in consequent text of the article. The SEM authentically illustrated structural changes when the molecules of different geometry and optimization are mixed closely with resin. The resin was semisolid and was very homogenously mixed with amino acids which are of zwitterionic structures and hence have shown effective activation energy changes on viscometric measurements. Of course, a little more inner chemistry is further modified due to molecular motions in three dimensions in form bond and atoms stretching and oscillations depicted by SEM pictures.

Surfaces under examination

The surfaces of the pure MFP resin are depicted in Figure 2(a) and are considered as reference surface for comparison of the surfaces of the blends of the MFP resin with additives. The MFP surfaces had undergone certain changes on blending with different additives due to their molecular activation and surface energies. Thus the ($\Delta\mu_2^*$) data are supplemented to explain surface modifications examined with SEM. The MFP surfaces were not fractured but kept intact. However on blending with additives, the MFP surfaces have undergone representational changes for geometric optimization due to stretching vibrations, molecular oscillations because the additives are heteroatom with electrostatic functional groups in their structure. The features are depicted in Figure 2(b–j). The chosen amino acids and surfactants are polar molecules, which developed specific interactions of resin with unique surface of the blends that was the result of intra and intermolecular forces which asserted for geometrical optimization in a form of intrinsic surface topography.

Physicochemical data

Densities of aqueous resin solutions (ρ_{aqs}) prepared, w/v, with Millipore water were measured[2] at 304.15 K $\pm$ 0.05°K. Viscous flow times (t) and pendant drop numbers (n) were noted with survismeter.[11] The density of pure resin (ρ_r) was determined with 5 mL relative density bottle (RDB) and Teflon cavity (TC) of 5 mL volumes. The resin was filled in 5 mL RDB, and in another RDB of similar capacity, the water was filled as reference liquid to same level as of the resin. The weights of empty RDB (W_e), with resin (W_r), and water (W_w) filled were noted for densities with eq. (1).

$$\rho_r = [((W_r - W_e)/(W_w - W_e)) + 0.0012(1 - ((W_r - W_e)/(W_w - W_e)))]\rho_w \quad (1)$$

The ρ_r and ρ_w are densities of resin and water, the 0.0012 is air density and $(1 - ((W_r - W_e)/(W_w - W_e))$ is a buoyancy correction in weights in air. The experiments were repeated with a cavity of fixed volume of Teflon (TC) due to nonsticking nature. The TC was absolutely dried in P_2O_5 filled dessicator for 24 h, and then was weighed and volume was determined by filling known volume of water which was measured with calibrated microburrete. A resin sample was filled in TC and weighed, for ρ_r eq. (2).

$$\rho_r = W_r/V_r \quad (2)$$

The V_r volume and W_r, the weight of resin calculated from $W_{TCr} - W_{TC}$ where the W_{TCr} the weight of TC plus resin and W_{TC} is weight of TC only. The ρ_r with both the methods were 0.7798×10^3 kg m^{-3}. The viscous flow times were measured for relative viscosities (η_r) with eq. (3).

$$\eta_r = \eta/\eta_0 = (\rho.t)/(t_0.\rho_0) \quad (3)$$

The η and η_0 are viscosities of solution and solvent, t and t_0 flow times, and ρ and ρ_0 are densities of solution and water, respectively.

Partial molal volume $\overline{V}_2^0$ and activation energy $\Delta\mu_2^{0*}$

The $\overline{V}_2^0$ was calculated as under.

$$\overline{V}_2^0 = [1000(\rho_0 - \rho)/m\ \rho_0\rho] + (M/\rho) \quad (4)$$

The M, molar mass of additives, ρ and ρ_0 are densities of solution and water. The $\overline{V}_1^0$ for water was 18.01/0.9953 = 18.09 cm^3 mol^{-1} at 304.15 K. the 18.01 is molar mass and 0.9953 the density of water.[3] The $\overline{V}_1^0$ and $\overline{V}_2^0$ data were used for activation energy calculation with eq. (5).

$$\Delta\mu_1^0 = RT\ln(\eta_0\overline{V}_1/hN) \quad (5)$$

The R is Rydberg constant, h is Planck constant, N is Avogadro's number, then

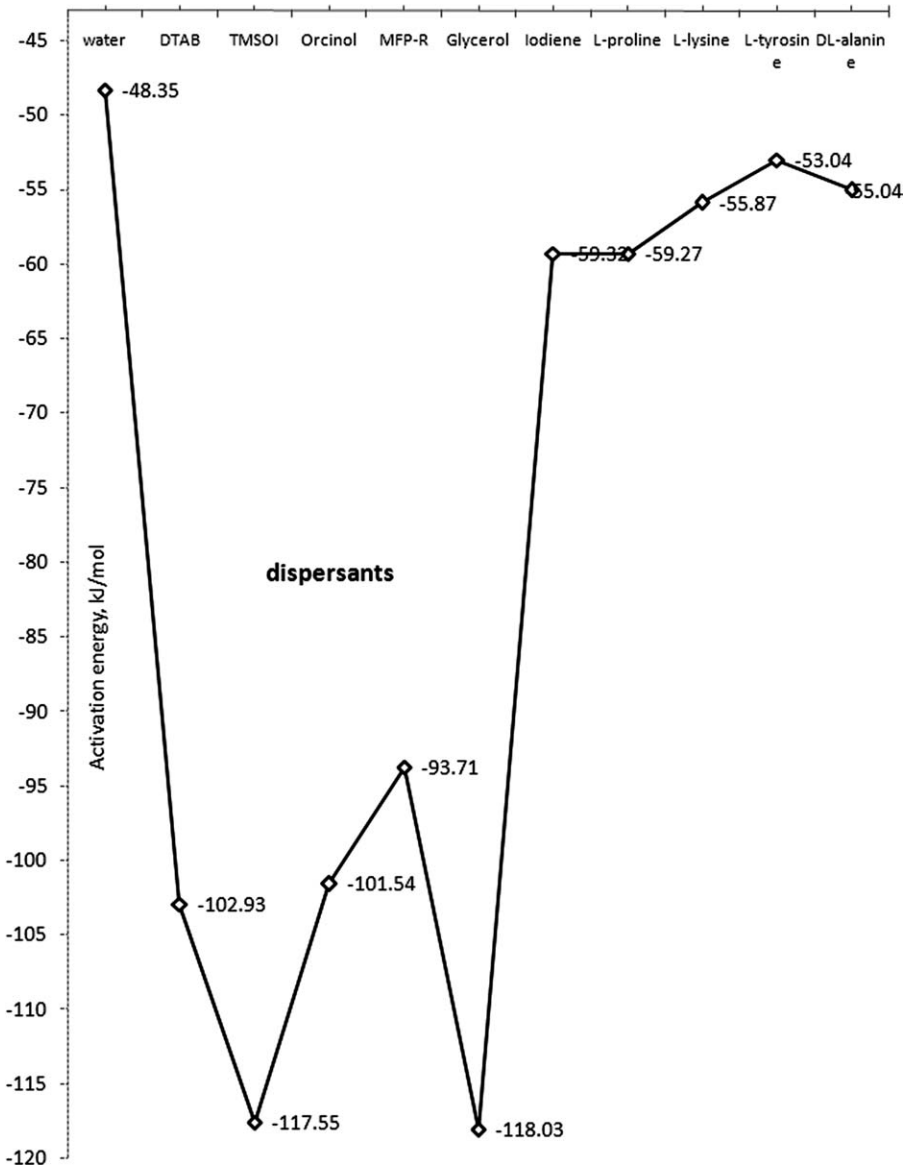

Figure 1 Activation energy ($\Delta\mu_2^*$, kJ mol^{-1}) of the additives.

$$\Delta\mu_2^{0*} = \Delta\mu_1^{0*} - (RT/\overline{V}_2)(1000\mathrm{B} - (\overline{V}_1^0 - \overline{V}_2^0) \quad (6)$$

RESULTS AND DISCUSSION

The $\Delta\mu_2{}^{0*}$data with negative values are as glycerol (−118.03) > TMSOI (−117.55) > DTAB (−102.93) > orcinol (−101.54) > MFP-R (−93.71) > iodine (−59.32) > L-proline (−59.27) > L-lysine (−55.87) > DL-alanine (−55.04) > L-tyrosine (−53.04) > water (−48.35) kJ mol^{-1} and plotted in Figure 1. The corresponding SEM micrographs are depicted in Figure 2.

The $\Delta\mu_2^{0*} < 0$, illustrated a state mixing of components together and define a level of structural mixing denoted with SEM micrographs. The negative $\Delta\mu_2^{0*}$ varied from 48.35 to 118.03 kJ mol^{-1} with a stronger structural reorientation assisted with several molecular motions, structural stretching, vibrations, translations, and oscillations. As mixing was not undertaken in any liquid state medium whereby solubilization and dissolution could play a role and hence molecular motions had played favorable role for mixing of the additives with MFP. A dynamics of mixing and microstructural variations were studied with the SEM and the $\Delta\mu_2^{0*}$ obtained in aqueous solution for estimation of a latent energy level of each additive and MFP individually were compared. The Figure 1 predicted a utilization of molecular energy for dispersal in aqueous medium with disruption of water hydrogen bonding. A maximum utilization of $\Delta\mu_2^{0*}$ with MFP was noted than glycerol and TMSOI were in a sequence due to hydrophilic and hydrophobic forces developed with hydrophilic functional groups and hydrophobic methyl groups.

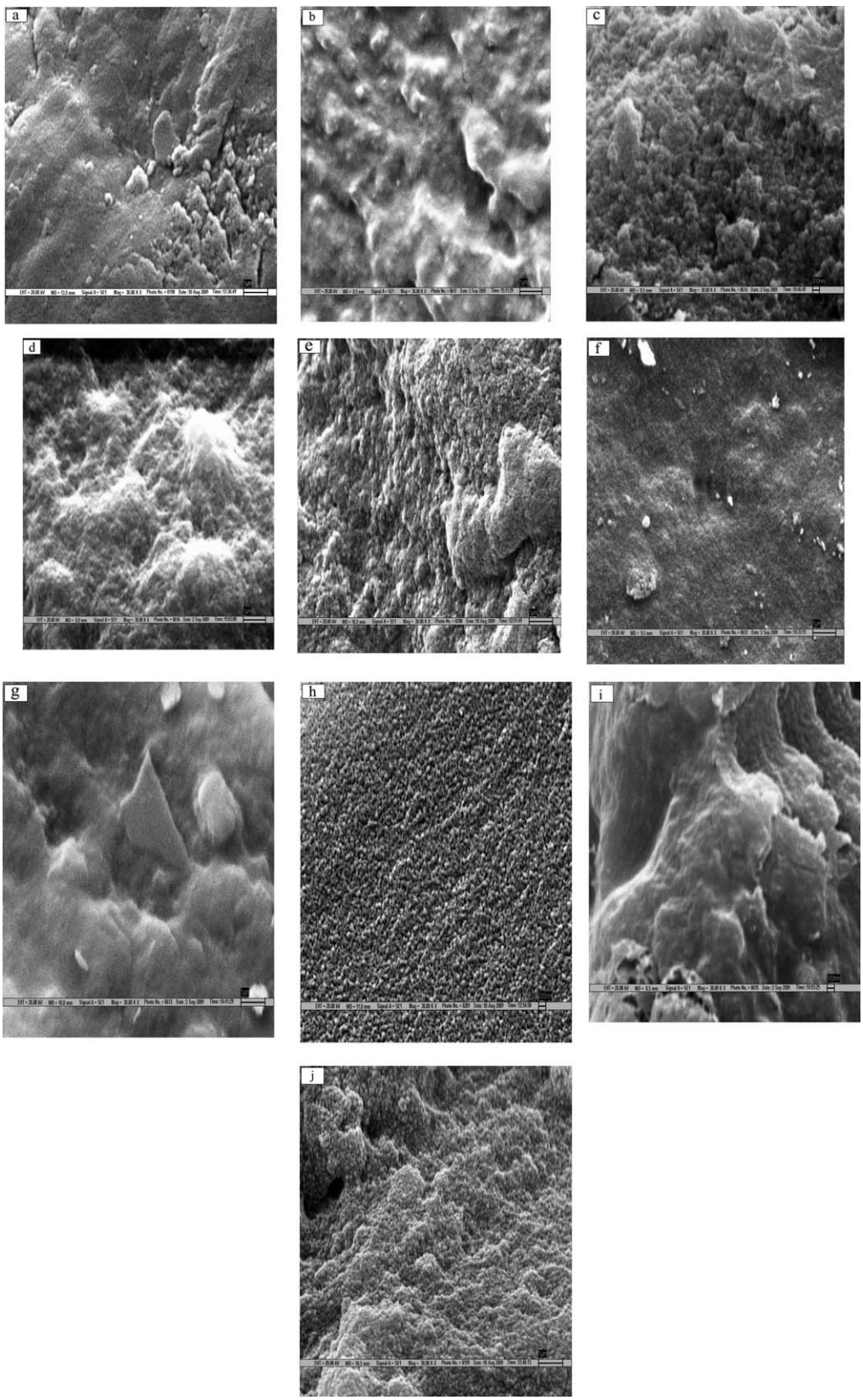

Figure 2 SEM images of the MFP pure and blend polymers (a–j). (a) Pure, (b) Glycerol, (c) L-Lysine, (d) DL-Alanine, (e) TMSOI, (f) DTAB, (g) L-Proline, (h) Orcinol, (i) L-Tyrosine, and (j) Iodine.

Thereby the MFP, glycerol, and TMSOI developed a homogenous solution by completely mixing. Additionally, the molecular oscillations, the vibrations and electronic potential (e^2/r), and the kinetic energy (½ mv^2) or momentum ($p^2/2m$) initiate activation to disperse the additives molecules among MFP molecular network (MNW). Similarly on a concept of Schrödinger equation, the $H\varphi = E\varphi$, in nutshell defined electromagnetic influence of the molecular motions. The Hamiltonian H represents all possible energy contributing factors and the E is a total molecular energy and the φ depicted a net area of electronic motions amplitude, which operationalized electrostatics and momentum as favorable factors to develop dispersion activities. The $\Delta\mu_2^{0*} < 0$, with utilization of $\Delta\mu_2^{0*}$ by additives are as glycerol > TMSOI > DTAB > orcinol > MFP-R > iodine > L-proline > L-lysine > DL-alanine > L-tyrosine > water, respectively with stronger hydrophilic of the glycerol and stronger hydrophobic of the L-tyrosine interactions.

The chemical potentials and dispersion energy $\Delta G = -nRTd$, the d is a dispersion constant, n moles, R constant, and T are a temperature in Kelvin. A variation in a SEM micrograph of MFP [Fig. 2(a)] with additives [Fig. 2(b–j)] had inferred operational effects on the $\Delta\mu_2^{0*}$. Hence the $\Delta\mu_2^{0*}$ data are highly relevant to elucidate microstructural variations depicted with the SEM of the blends. Thereby, a correlation for the $\Delta\mu_2^{0*}$ was established with SEM, which very rightly explained a thermodynamics condition for mixing of the L-lysine, L-tyrosine, L-proline, DL-alanine, glycerol, orcinol, iodine, DTAB, and TMSOI on a pattern of $\Delta\mu_{2(\text{dispersion})} < 0 > \Delta\mu_{1(\text{reversal})}$.

SEM was recorded noncryogenically

The temperature of blending is depicted in the text and blending was at hot melt of resin and 1 atmospheric pressure, and the surfaces were maintained at NTP. No cryoscopy techniques were applied in fact it was avoided to prevent unnecessary shrinking of the molecular sizes, which could have been a hindrance in blending. The cryoscopy is not suitable to blending chemistry and composites.

The molecular electrostatics has been a ground to explain a state of activation, reportedly the glycerol with 3-OH hydrophilic and 3 C atoms carbon chain with hydrophobic caused a maximum molecular energy utilization (Fig. 1) where the $\Delta\mu_2^* < 0$ is indicator of mixing with MFP resin. The MFP resin has heteroatomic core of melamine ring bridged with PVP molecule via —N<(CH_2—O)$_2$>C< attachment. The MFP molecular networks was fixed and structures of a dispersant was variable [Fig. 2(a)]. For example, the glycerol is with 1 : 1 ratio of hydrophilic and hydrophobic interactions, which was compared with the TMSOI [Fig. 2(b–e)]. The TMSOI has also 3 : 3 → 1 : 1 ratios of the hydrophilic to hydrophobic interactions. The 3 CH_3 groups developed the hydrophobic and the $O^-= S^+–I^-$ partially charged three atoms caused the hydrophilic interactions, with stronger molecular interaction potential and stronger intermolecular forces. The atomic oscillations do make a dent in the MFP molecular structure, which is depicted by SEM images. The molecular structure of DTAB with 12 C atoms alkyl chain plus 3 CH_3 groups, which developed the hydrophobic interactions but N^+-Br^- atoms developed the hydrophilic interactions. So in case of the DTAB, the hydrophobic interaction dominance has shifted the ratio to hydrophobic over hydrophilic where the hydrophobic has utilized lower $\Delta\mu_2^*$. The DTAB's SEM showed a globular structure [Fig. 2(f)] differed from the glycerol and TMSOI. The orcinol as compared to the DTAB further weakened the $\Delta\mu_2^{0*}$ of the MFP with lower intermolecular force due to π conjugation in orcinol benzene ring, which further reduced utilization of $\Delta\mu_2^*$ with weaker mixing [Fig. 2(h)]. However, orcinol being a smaller molecule distributed homogenously with a dewetting phenomenon and MFP alone further lower $\Delta\mu_2^*$ utilization with slightly prominent ridges with the $\Delta\mu_2^* = -48.35$ kJ mol^{-1}, which inferred a stronger hydrophobic where the $\Delta\mu_2^*$ value is decreased with weak molecular interaction potential and intermolecular forces. Apart from these the I_2 showed weaker mixing where of interstitial arrangement of I_2 into MFP void spaces is noted in SEM [Fig. 2(j)]. A comparison of a SEM of the MFP with that of the MFP + I_2 depicted this difference with interstitial features [Fig. 2(a–j)]. The amino acids very weakly dispersed with MFP, for example, the L-proline with free —COOH group, its O atoms used less $\Delta\mu_2^*$ with poor symmetric dispersion depicted in SEM [Fig. 2(g)]. The other amino acids further lowered use of $\Delta\mu_2^*$ with weaker molecular interaction potential and intermolecular force, for example the L-lysine with four carbon atoms, alkyl chains, 2-NH_2, and 1 COO^- groups in a linear manner reduced a consumption of the $\Delta\mu_2^*$. Its SEM showed a rocky image with weaker binding or cohesive energy and adhesive force [Fig. 2(c)]. The L-tyrosine with benzene ring, with —OH and linear chain with 2 C atoms where —NH_2 and COOH are attached, which weakened the effects and was not able to develop either hydrophilic or hydrophobic. So no more use of a $\Delta\mu_2^*$ folder or bolder are noted in SEM [Fig. 2(i)]. The DL-alanine with 1 C atom and 1 CH_3 group and at as NH_2 and COO^- compared but hydrophilic stronger and hydrophobic weaker so as compared to L-tyrosine use more $\Delta\mu_2^*$ with higher symmetry in SEM images [Fig. 2(d)]. As the unshared pair of electron on O atoms had higher energy as compared to the shared electron, hence

develop higher oscillations. These oscillations approached the void spaces of MFP structure and oscillate MFP atom based on collision theory.

SEM of blend and pure MFP

No sputter coating was attempted as the resin was semisolid and additives were in powered form and quickly blended. Their activation energies supported their quicker blending process. In general, sputtering coat is in case of solid and power forms of the substances. Both the components showed favorable tendency to mix mutually depicted by SEM. It was a case of bulk blending, not surface coating, where no sputtering coat is used. No stain was used as it was a bulk blending not a surface mixing. As the bulk blending was made and the SEM sections clearly depicted the internal morphology of the material. The similar concept was applied in our studies where the comparative SEM studies of different blends samples were made. No topography was focused except the blends features and physicochemical changes. The SEM preparation method or sample mounting method was the same to each sample and hence point of artifacts is not possible. As each macromolecule has its own optimization and reorientation on the basis of its intra and intermolecular forces. Hence the SEM is most effective technique as micro molecule to depict the same and it has been a basis of our studies. Each additive with different molecular structure depicted different SEM. The SEM is an effective indicator in nanotechnology to identify the nano level changes at molecular level. Hence the SEM pictures depict in Figure 2(a–j) authentically inferred an effect molecular mixing of MFP and amino acids along surfactants. The immiscible polymers blends develop microphases and depict the phases of two molecules confined to respected phases. Here staining was not effective as our blends were at bulk level not at solid–liquid basis. The MFP aqueous solutions were studied for viscometer; we conducted which are Newtonian liquids. The $\Delta\mu_2^{0*}$ was derived from intrinsic viscosity data given in reference.[10]

Pure MFP resin

A microstructure of the MFP is with crustations with specific arrangement of polyvinyl chain (PVC). Also the smaller extensions of pyrrolidone ring are noted along rocky crustation whose partitions are distinguished with sutures [Fig. 2(a)]. The crustation is noted to come out in a form basal parts, which seem to be a melamine ring. The 3 N atoms out of ring of the melamine, which are out of benzene ring seem to be operational. Perhaps these 3 N atoms establish a bridge with O atoms of a bridge and developed stronger intermolecular forces [Fig. 2(a)]. It showed a smooth surface, stronger and compact packing of atoms and molecules of the resin. The smooth surface area indicates extensive intermolecular bonding, might be due to crosslinking within the molecule.

Nonbrittle surfaces

The surfaces were in continuous and not brittle as the resin was in a semisolid state, which is a most suitable state of controlled blending with mediocre level of the intermolecular forces. The samples were maintained in airtight container. Also the intrinsic viscosity data were derived from 7 to 9 samples of their aqueous solutions of different compositions for calculation of the activation energies. The measurements made with survismeter showed a continuous flow of the solutions.[10] The detailed data including surface energy in J/m^2 are reported elsewhere.[10] Similarly, the SEM pictures of the MFP also prove nonfractured surfaces. Our activation mu2 referred mixing thermodynamics of the bulk phases.

Glycerol

The glycerol brings an equal molecular distribution [Fig. 2(b)] where the $e^{-E/Kt}$ (electrostatic) and kinetic potential ($P^2/2m$) rendered an assistance in equal distribution of the glycerol molecules. The kinetic potential is operational and as per BoltzMann distribution law, the equal hydrophilic and hydrophobic forces of the glycerol optimize the MFP resin. The glycerol [Fig. 2(b)] is compared with the structure shown in Figure 2(a) with higher uniformity. It seems that the glycerol blending with MFP is very useful for physicochemical superiority of the resultant resin. A uniform and smooth surface is noted due to symmetric molecular interactions with an extent of hydrophilic forces between the resin and glycerol (Fig. 2(b)].

L-Lysine

When L-lysine was blended with the MFP, the prominent furrows with stronger up rising ridges were noted [Fig. 2(c)]. Because the alkyl chain with 4 C atoms where terminal $-NH_2$ turns back and interact with carboxylic groups as the L-lysine has two amino groups. These amino groups twist the molecule to develop hydrogen bonding with O atoms of the MFP resin and probably —OH of the L-lysine developed bonds with melamine N atoms.

DL-Alanine

DL-alanine structure is noted with a superfine fibrous structure which is very near to glycerol blend. The carboxylic and amino groups developed the hydrophilic

and the CH_3, CH, the hydrophobic where the hydrophilic interactions are stronger and bound strongly with the MFP resin [Fig. 2(d)]. The images are with some porosity as well as smoothness, due to interaction between the resin and the DL-alanine. As compared to glycerol the smooth surface is lost due to intermolecular attraction between the resin and the amino acid which is of moderate level.

TMSOI

TMSOI developed a granular superfine structure where I_2 with induced potential of the O and the S polar atoms are fitted with resin suitably and the 3 CH_3 of the TMSOI are an engulfed where PVP chain is freely hanging. With TMSOI [Fig. 2(e)], the surface became porous, with a loss of smoothness due to intermolecular interaction between the resin and TMSOI. Perhaps the interactions are not so strong, thereby porous structure and smooth surface to some extent are developed. It developed a very highly symmetric microstructure with few globules like oil–water.

DTAB

The DTAB with 12 C atoms is properly filled with PVC and developed a uniform thin film with continuity micrograph. The DTAB surface seems to be very smooth with no porosity with almost even surface, with stronger binding forces between the resin and the DTAB [Fig. 2(f)].

L-Proline

The L-proline showed unique microstructure with few folders. Perhaps pyrole rings of the L-proline were fitted in the resin structure, and carboxylic group developed stronger hydrophobic interaction force with resin [Fig. 2(g)].

Orcinol

The orcinol highly compact microstructure was noted where 1 CH_3, 2 OH groups and one benzene ring are exclusively fitted with MFP and formed a highly thin film. The Figure 2(h) was clearly showed a granular, even/symmetric surface, with similar interaction force between the resin and orcinol molecules. The granular structure may be due to the constant interaction force between the orcinol and the resin molecules. The addition of orcinol with resin made the surface morphology from smooth to highly granular form.

L-Tyrosine

The L-tyrosine depicted a more crustation form with weaker hydrophilic and stronger hydrophobic forces with one benzene ring and 1 OH groups of the L-tyrosine [Fig. 2(i)]. The smooth and highly unsymmetrical structure is noted with stronger interaction force between the resin and L-tyrosine along stronger intermolecular forces of the attraction between the amino acid and resin. The extent of binding was higher [Fig. 2(i)], hence the iodine blend showed rocky surface as compared to the pure resin [Fig. 2(j)]. The surface became uneven and unsymmetrical with higher porosity.

Iodine

The iodine developed stronger hydrophobic interaction and weaker hydrophilic interaction as the iodine is a least stable with induced electropositive charge. Therefore it developed stronger hydrophilic intermolecular forces [Fig. 2(j)].

Significance of study

Significance of SEM spectra is useful for material development with industrial features. The $\Delta\mu_2^{0*}$study offers information on oscillations and deformation in original framework of MFP with additives to identify the blends for several molecular functions adsorbent and binding of toxic metals. The SEM spectra have successfully illustrated the bulk structure for molecular distribution for successful combinations and simulations of resin depicted in [Fig. 2(a–j)]. The blends of L-proline, L-tyrosine, glycerol, DTAB, iodine, TMSOI, L-lysine, DL-alanine, and orcinol slightly differed from each other with molecular oscillations. The micrograph has revealed that the orcinol is deeply embedded in MFP matrix and enhanced and inhibited a MFP. In case of TMSOI blend, the rocky structure is seen due to enlargement of resin with an increase in temperature. With a granular mode with orcinol, had established the stronger hydrophilic interaction whiles the iodine, TMSOI, L-lysine, DL-alanine, orcinol weaker. The N atoms and a benzene ring in a resin introduced such behavior.

CONCLUSION

Aqueous MFP resin solution was noted as nonNewtonian solutions with shear stress on laminar flow. The L-proline, L-tyrosine, glycerol, DTAB; and iodine, TMSOI, L-lysine, and DL-alanine blends had reasonable similarity in morphology as smooth, rocky, granular surfaces but much granular microstructures are noted with the orcinol.

Authors are thankful to the textile and polymer department-IIT, Delhi, for SEM, Dr. A.S. Sarpal and Dr. J. Christopher-

Indian Oil Corporation, Faridabad, Haryana, for fruitful discussion and Dr. A.P. Raste, Principal, Deshbandhu College, Delhi University for infrastructural supports.

References

1. Bakshi, M. S.; Kaura, A.; Kaur, G. J Colloid Interface Sci 2006, 296, 370.
2. Singh, M. Phys Chem Liq 2008, 46, 98.
3. Singh, M.; Sharma, Y. K. Phys Chem Liq 2006, 44, 1.
4. Valery, C.; Pouget, E.; Pandit, A.; Verbavatz, J. M.; Bordes, L.; Boisde, I.; Cherif-Cheikh, R.; Artzne, F.; Paternostre, M. Biophys J 2008, 94, 1782.
5. Hafner J, J. Mol Struct 2003, 3, 651.
6. Elliott, R. S.; Shaw, J. A.; Triantafyllidis, N. J Mech Phys Solids 2006, 54, 193.
7. Konozenko, I. D.; Ryzhkov, Y. T. J Mater Sci 1968, 2, 425.
8. Rossnagel, K.; Smith, N. V. Phys Rev B 2006, 73, 073106.
9. Bartschat, K. J Phys B: At Mol Opt Phys 1992, 25, L307.
10. Singh, M.; Kumar, V. J Appl Polym Sci 2009, 114, 1870.
11. Singh, M. J Biochem Biophys Methods 2006, 67, 151.